

Effect of fibers and welded-wire reinforcements on the diaphragm behavior of composite deck slabs

Salah Altoubat ^{*1}, Hisseine Ousmane ^{2a} and Samer Barakat ^{1b}

¹ Department of Civil & Environmental Engineering, University of Sharjah, P.O. Box 27272, Sharjah, UAE

² Department of Architectural Engineering, University of Sharjah, P.O. Box 27272, Sharjah, UAE

(Received April 30, 2014, Revised November 13, 2014, Accepted December 29, 2014)

Abstract. Twelve large-scale composite deck slabs were instrumented and tested in a cantilever diaphragm configuration to assess the effect of fibers and welded wire mesh (WWM) on the in-plane shear capacity of composite deck slabs. The slabs were constructed with reentrant decking profile and reinforced with different types and dosages of secondary reinforcements: Conventional welded wire mesh (A142 and A98); synthetic macro-fibers (dosages of 3 kg/m³ and 5.3 kg/m³); and hooked-end steel fibers with a dosage of 15 kg/m³. The deck orientation relative to the main beam (strong and weak) was also considered in this study. Fibers and WWM were found efficient in distributing the applied load to the whole matrix, inducing multiple cracking, thereby enhancing the strength and ductility of composite deck slabs. The test results indicate that fibers increased the slab's ultimate in-plane shear capacity by up to 29% and 50% in the strong and weak directions, respectively. WWM increased the ultimate in-plane shear capacity by up to 19% in the strong direction and 9% in the weak direction. The results suggest that discrete fibers can provide comparable diaphragm behavior as that with the conventional WWM.

Keywords: steel decking; composite slab; fiber-reinforced concrete; diaphragms; in-plane shear

1. Introduction

The use of composite deck slabs has become a preponderant practice in today's construction industry and arguably almost all steel-framed buildings are constructed using this type of flooring system. A typical composite deck slab consists of a profiled steel sheet, a concrete topping, and a welded wire mesh (WWM). The profiled steel sheet serves as a construction platform and as a permanent formwork for the fresh concrete. It also serves as the main tensile reinforcement for the concrete during service; hence, theoretically no additional steel is needed for flexural strength purposes. Composite deck slabs often function as diaphragms in multistory buildings to transfer in-plane shear forces induced by wind and seismic loads to adjacent lateral load-resisting elements. Consequently, the diaphragm behavior of composite deck slabs has recently become a concern to structural engineers. For the last few decades, the flexural behavior of composite deck slabs has

*Corresponding author, Associate Professor, E-mail: saltoubat@sharjah.ac.ae

^a Lecturer, E-mail: hahmad@sharjah.ac.ae

^b Professor, E-mail: sbarakat@sharjah.ac.ae

been widely researched (Easterling and Young 1992, Abdullah and Easterling 2007, Lopes and Simões 2008, Hedaoo *et al.* 2012) and guidelines for the design of composite deck slabs have been established (ASCE 1992, EC4 2001). However, the extent of research works - in the open literature - focusing on the behavior of composite deck slabs in diaphragm action has been quite scarce. Some research studies on diaphragm action have been conducted by some steel-deck manufacturers since 1960s, especially in the USA and Western Europe, but the outcomes of these studies haven't been widely published for their proprietary nature.

The importance of diaphragm action of composite deck slabs becomes more pronounced in light of the recent trend in using discrete fibers as a secondary reinforcement for composite deck slabs in lieu of the conventional WWM. In effect, the WWM in composite deck slabs is essentially used to control rather than prevent the cracks associated with restrained shrinkage and temperature changes in concrete and has hypothetically no flexural role. Thus, recently discrete fibers have emerged as an alternative secondary reinforcement in this application.

Recent studies on fiber-reinforced concrete have demonstrated the ability of discrete fibers to overcome the inherent brittleness of concrete and thus to enhance its residual strength, toughness and ductility, which makes fiber-reinforced concrete an attractive material for a range of applications including composite decking (Roesler *et al.* 2006). Tantamount, recent investigations on the flexural behavior of fiber-reinforced composite deck slabs have proved the adequacy of fiber as an alternative secondary reinforcement to the traditional wire mesh in composite deck slabs (Guirola 2001, James and Easterling 2006). However, there are concerns over the behavior of fibrous composite deck slabs under in-plane shear. The present research is intended to address such concerns.

In general, the review of available relevant literature reveals that the major factors dictating the diaphragm capacity consist of the profile and sheet thickness of the steel deck; the orientation of deck corrugations; the strength and arrangement of shear connectors; the shear transfer mechanism; the strength of concrete topping; and the secondary reinforcement system.

Luttrell (1971) investigated the effect of both concrete topping and edge connectors on the diaphragm capacity of composite deck slabs in a set of nine diaphragm tests. He used steel decking of trapezoidal profile with lightweight concrete topping and welded connections. The stiffness and ultimate loads of the diaphragms were compared to similar diaphragms without concrete topping. Considerable increase in strength and ultimate load were obtained as the topping increased the stiffness of the diaphragm and forced the failure to take place at the welds (Connection failure). Expressions correlating diaphragm strength to the number of diaphragm edge welds were developed.

Davis and Fisher (1979) carried out large-scale tests on composite deck slabs using trapezoidal and reentrant decking profiles attached to the edge frame through self-drilling, self-tapping screws. They established formulas for diaphragm capacity based on assumptions regarding the force distribution on the fastener pattern. However, since frequently composite deck slabs in practical conditions are connected to the building frame through headed shear studs, the applicability of those formulas are limited to specific connector type and arrangement.

The effect of connector arrangement on the in-plane shear strength of composite walling was also addressed by Hossain and Wright (2004) who conducted small-scale tests of one-sixth scale. They formulated an analytical model for the shear strength of composite walls based on analogy to composite deck slabs. However, the axial load component in composite walling implies a completely different shear transfer mechanism.

Easterling and Porter (1988, 1994) presented a comprehensive study on composite deck slabs

through their research involving the testing of 32 full-scale composite diaphragms. Three failure limit states were identified based on the test results: The diagonal tension, the edge connector, and the shear transfer mechanism. Analytical models predicting diaphragm capacity were also formulated. However, since no secondary reinforcements were used, test results showed that at the post-peak phase, all diaphragms exhibited brittle inelastic behavior with increasing in-plane displacement.

The effect of shear transfer mechanism on the strength of composite deck slabs and its impact on the deterioration of the interfacial bond between the steel deck and the concrete topping have been addressed by several recent investigators. In most of the cases, additional to the horizontal shearing forces, the bending action also leads to vertical separation between the steel and the concrete (Chen *et al.* 2011, Saravanan *et al.* 2012, Cifuentes and Medina 2013). However, generally those investigations focused on the horizontal shear resulting either from bending or cyclic loading. Hence, sufficient information relevant to shear transfer mechanism in diaphragm application of composite deck slabs is still lacking in the literature.

On the other hand, the effect of secondary reinforcement on the in-plane shear behavior of composite deck slabs has rarely been investigated, and thus the behavior of composite deck slabs under in-plane shear when the conventional mesh is replaced with fibers remains nebulous. The contribution of the secondary reinforcement toward the shear capacity is rarely considered in the design of composite deck slabs, although its presence is a plus and some designers would consider it in the computation of the in-plane shear strength of composite slabs when the capacity of the concrete core alone is marginal. The present study aims to shed the light on the diaphragm behavior of fiber-reinforced composite deck slabs through an experimental program in which the in-plane shear performance of fibrous composite deck slabs are compared to that of composite deck slabs reinforced with conventional WWM.

2. Experimental program

2.1 Test setup description

A test rig was exclusively designed to test cantilever diaphragms in this research and is shown in Fig. 1. It consists of a slab support and a reaction frame. The slab support consists of a reaction beam that provides the fixed-end condition of the cantilever diaphragm and rollers on the opposite side to support the free-end of the diaphragm against out of plane loads. This allows for in-plane movement while reducing out of plane effects due to self weight of the slab. The reaction beam consists of a built-up steel beam of 3000 mm length and 840 mm depth. The depth of 840 mm was carefully selected in order to allow for an easy access from the bottom side during installation, instrumentation and removal of the slabs. The bottom flange of the beam is attached to the rigid floor of the laboratory through a set of 18-high strength bolts. The top flange of the beam has four rows of holes used to fix the shear connectors embedded inside the testing slab and thus provide the fixed-end condition of the diaphragm.

The reaction frame consists of a main 2500 mm long built-up steel column to which a 500 KN actuator is attached. Three lateral braces were attached to the main column to enhance its lateral stability. The specimen shown in Fig. 1 is for the strong orientation; however the same setup can be used to test the weak configuration by having the corrugation spanning parallel to the reaction beam. In this case, each row of shear connectors will be placed in one longitudinal trough of the steel profile parallel to the beam.

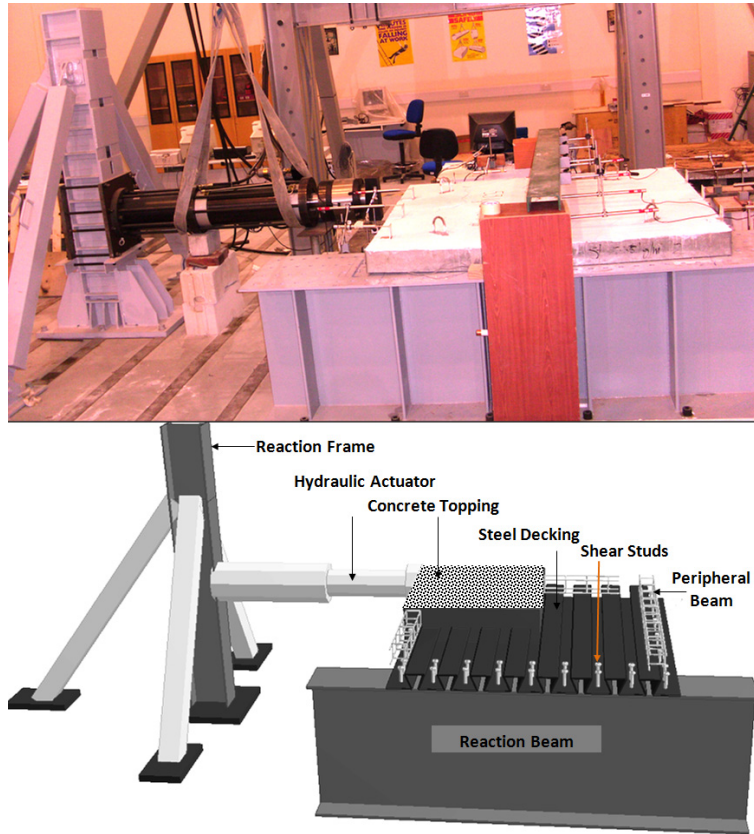


Fig. 1 Test rig

2.2 Material properties

2.2.1 Synthetic fibers

The main components of the synthetic macro fiber used in this project are polypropylene and polyethylene (Fig. 2(a)). The fiber has geometry and mechanical properties that enhance dispersibility in the concrete mix. It is rectangular in shape with a nominal length of 40 mm; an average width of 1.4 mm; an average thickness of 0.105 mm; and an aspect ratio of 90. The fiber has a tensile strength of 620 MPa and a modulus of elasticity of 9.5 GPa.

2.2.2 Steel fibers

The steel fiber used in this project consists of cold drawn wires with hooked ends (Fig. 2(b)). The wires are lumped in bundles by an adhesive that dissolves during the mixing process and ensures an easy mixing and homogeneous distribution. The fiber is 60 mm long, 0.9 mm in diameter and has an aspect ratio of 65. It has a tensile strength of 1000 MPa and a modulus of elasticity of 200 GPa.

2.2.3 Weld Wire Mesh (WWM)

Two common sizes of WWM (Fig. 2(c)) made of S500 steel (yield strength of 500 MPa) were

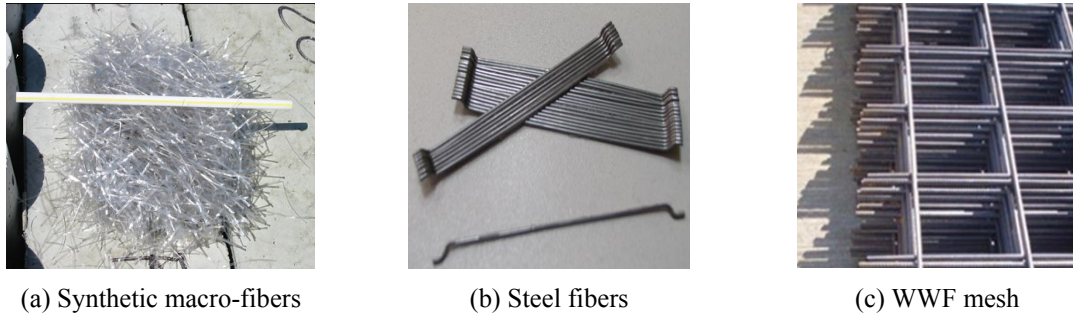


Fig. 2 Secondary reinforcement in composite slabs

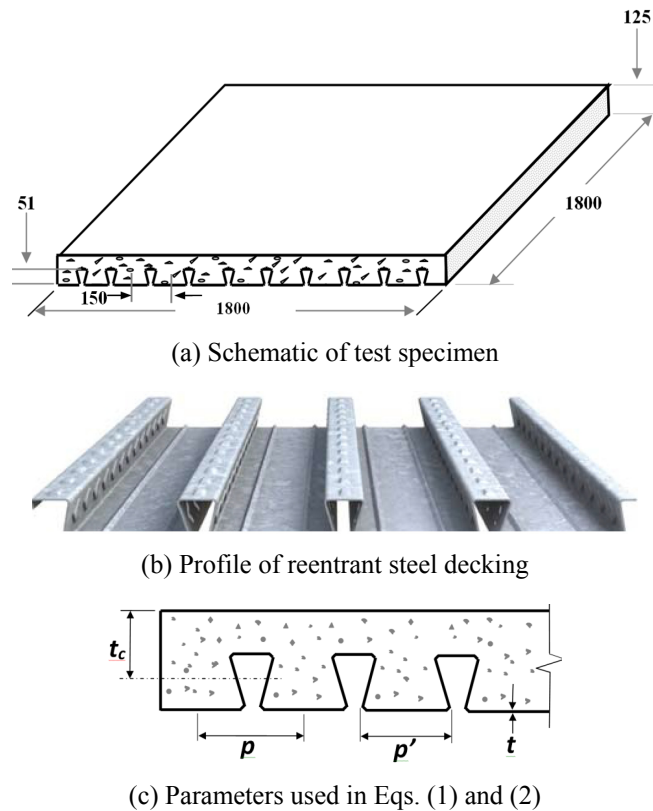


Fig. 3 Test Specimen and geometry of decking profile

used: A98 and A142 with steel bar diameter of 4 mm and 6 mm, respectively, and steel area in each direction equivalent to 98 mm²/m and 142 mm²/m, respectively.

2.2.4 Steel decking

A reentrant steel decking profile with a depth of 51 mm and a rib spacing of 150 mm was used (Fig. 3). The steel sheets are manufactured from a material conforming to the specifications of BS EN 10147-S350 GD+Z275-N-A-C (reaffirmed 2000), namely hot-dip galvanized, with minimum

yield strength of 350 MPa. Fig. 3(c) shows schematic notations for the deck slab parameters that are used to determine the effective thickness of the composite slab as described later in Section 3.3.

2.2.5 Shear connectors

This project used headed stud shear connectors with yield strength of 580 MPa, compliant with the requirements of BS EN ISO 898 (reaffirmed 2009).

2.3 Concrete mixture

Four concrete mixes with targeted compressive strength of 40 MPa were used. The mixture proportions and mix properties are provided in Table 1. The maximum aggregate size used was 20 mm. The coarse aggregate used had a specific gravity of 3.10. The fine aggregates consist of natural washed sand and crushed stones with specific gravities of 2.62 and 2.50, respectively. The mix designs were adjusted in order to accommodate the addition of fibers by limiting the coarse to fine aggregate ratio to 55% of the total volume of aggregates as per ACI guidelines (ACI 544.3) (reaffirmed 2011). The concrete mixes were supplied from the ready mix plant in batches, and for each concrete batch, cube samples were prepared and tested according to BS 1881-101 (1983) and BS 1881-116 (1983), respectively. Additional beam samples were cast to measure the residual flexural strength of the FRC mixtures. The average values of the equivalent flexural strength, $f_{e,3}$, measured according to JSCE guidelines (JSCE-1984) at 3 mm deflection were also reported in Table 1 (based on testing six standard beam specimens), which can be obtained from bending of beams under third-point loading with a support span of 450 mm. The equivalent flexural strength, $f_{e,3}$, is calculated by inserting the average load into the formula for the modulus of rupture. The average load is equal to the area under the load versus deflection curve (also called toughness) measured up to a beam deflection of 3 mm divided by 3 mm. The $f_{e,3}$ value is directly proportional to the toughness value T_{150}^{150} defined in the ASTM guidelines (ASTM C1609-07) - flexural beam test, using a 150 mm by 150 mm by 550 mm beam. The $f_{e,3}$ value as well as the T_{150}^{150} value are directly proportional to the area under the load-deflection curve up to a central beam deflection of 3 mm.

Table 1 Mix proportions and concrete properties

Material (kg/m ³)	Mix 1	Mix 2	Mix 3	Mix 4
Cement OPC	380	380	380	380
20 mm aggregate	630	630	630	630
10 mm aggregate	440	440	440	440
Fine aggregate	880	880	880	880
Free water, L	196	200	200	200
Super plasticizer, L	0.50	1.50	1.50	1.50
Water cement ratio	0.52	0.53	0.53	0.53
Coarse to fine aggregate ratio (by volume)	0.54	0.54	0.54	0.54
Synthetic fiber	-	3.0	5.3	-
Steel fiber	-	-	-	15.0
Average cube compressive strength, MPa	46.8	41.9	45.8	43.6
Equivalent flexural strength ($f_{e,3}$), MPa	-	1.4	2.2	1.5

2.4 Test specimens

Twelve composite deck slabs with a cantilever diaphragm configuration were constructed and tested under in-plane monotonic loading to failure. The slabs were (1800 mm × 1800 mm × 125 mm) and were constructed using reentrant steel decking profile of 0.9 mm sheet thickness (Fig. 3). The slabs were attached to the reaction beam through two rows of 16 mm diameter shear connectors embedded into the concrete slab and bolted to the flange of the reaction beam. The shear connectors were spaced at 150 mm in both strong and weak directions in compliance with AISC guidelines (AISC 2001). The strong orientation is defined as when the deck corrugations are perpendicular to the main beam (the reaction beam), while the weak orientation is when the deck corrugations are parallel to the main beam. A small peripheral reinforced strip was used at the free edges of the slab to provide rigidity to the diaphragm, to circumvent local failure at the point of load application, and to force failure to occur within the slab (Fig. 4(a)). The effects of fibers (synthetic and steel) as well as that of the deck orientation were examined. Eight slabs were tested in the strong direction, and four slabs were tested in the weak direction. The assortment of different reinforcement systems used for the different slabs is presented in Table 2. All the specimens were instrumented with embedded and external strain gages to capture the strain in the concrete and the steel deck at selected key locations. Linear Voltage Displacement Transducers (LVDTs) were mounted along the centerlines and the edges of each slab to record the in-plane deflection of the specimen.

2.5 Instrumentation and testing

The composite metal deck slabs were instrumented with embedded and external strain gages to monitor the strain in the concrete and in the steel deck at different stages of loading. The embedded strain gages used to capture the strain in the concrete are of type Vishay EPG-5-350Ω with a length of 100 mm and were laid out as illustrated in Fig. 4(a). Three of the gages were placed at equal spacing along the diagonal of the specimen at the slab mid-height, perpendicular to the potential direction of a diagonal crack; and one gage was attached off-diagonal at a location where a potential flexural crack could occur. Another type of strain gages (surface mounted) of type Tokyo Sokki TML-120Ω with a length of 10 mm and a gage factor of 2.1 were attached in pairs but at different levels. The first was attached at the surface of the steel deck at the interface between the concrete topping and the steel deck, while the second was attached at the top surface of the concrete slab as shown in the layout in Fig. 4(b). For every pair of strain gages of this type, the first number in the label refers to the gages attached on the steel deck, while the second refers to the one attached on the top surface of the concrete topping. The measurements obtained from these strain gauges were used to evaluate the composite action in the slabs and the load at which debonding possibly occurs.

A total of 12 LVDTs were used to record the in-plane deformation of the slab: Four of them were placed at the slab corners, and eight were mounted at equal spacing along the slab edges and center lines. A data acquisition system was used to collect the strain and deformation data during all the stages of testing. The slabs were tested in displacement control mode with a displacement rate of 0.02 mm/sec. The load was applied to the slab using a 150 mm × 150 mm rigid steel plate to distribute the point load on the composite slab and to engage both the steel profile and concrete topping in carrying the load. The measured parameters in the test were: the in-plane loads and deformations; the strain at key locations in the concrete, the steel deck, and the interface between

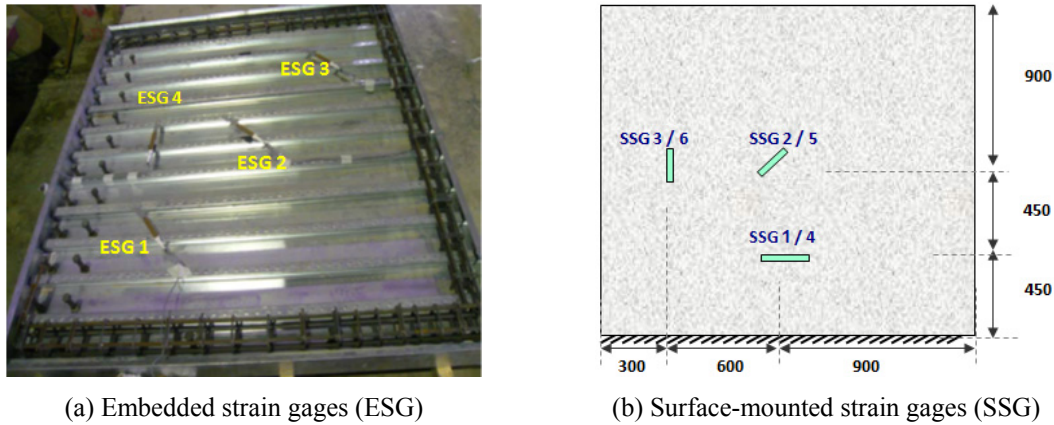


Fig. 4 Arrangement of strain gages

the steel deck and the concrete. The ultimate load carried by each slab, the load versus in-plane deflection response, and the load-strain response were used to evaluate the effect of different secondary reinforcement systems on the in-plane shear behavior of composite deck slabs.

3. Results and discussions

3.1 Load-deflection results

3.1.1 Weak configuration

Due to the slight variation in the concrete compressive strength between the different slabs, the experimental test results including the ultimate load were normalized to the concrete compressive strength for the control specimen in each set using a normalization factor proportional to the square root of the compressive strength. The normalized in plane load-deflection curves for the slabs tested in the weak direction are presented in Fig. 5. The diaphragm strength in the weak direction is important to evaluate since the in-plane shear developed in the diaphragms is in both directions. The concrete topping plays a vital role in the weak direction as the shear strength of the diaphragm depends highly on the concrete topping above the deck flute. The load deflection curves illustrate that the control slab exhibited the lowest ultimate in-plane shear capacity (144 KN) followed by a substantial drop in the load carrying capacity and a rapid degradation in the post-peak strength. The slab reinforced with A142 mesh showed slightly improved ultimate and post-peak strengths relative to the control slab, but it also experienced some degradation in the post-peak load carrying capacity.

On the other hand, the slabs reinforced with synthetic macro-fibers (5.3 kg/m^3 and 3.0 kg/m^3) exhibited greater ultimate load and sustained the ultimate load for a wider range of in-plane deformation relative to the control slab. Additionally, they exhibited a smooth and stable post-peak behavior and thus showed superior performance to that with the conventional WWM in terms of strength and ductility as shown in the load deflection response. This suggests that, in the weak configuration of composite deck slabs, the slabs reinforced with macro synthetic fiber at the tested dosages provide higher in-plane shear capacity and ductility than that with the tested WWM.

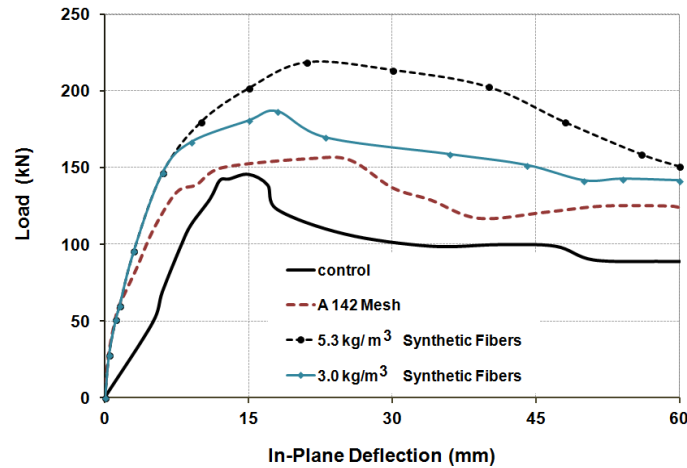


Fig. 5 Load-deflection response for slabs tested in the weak direction

3.1.2 Strong configuration

The normalized load deflection curves for the slabs tested in the strong direction are represented in Fig. 6 for the different types of secondary reinforcement systems. The results showed that all slabs exhibited a linear response until the first diagonal tension crack was initiated. The initiation of the first diagonal tension crack was marked by a change in the slope of the load deflection curve after which two distinguished behaviors were observed. The control slab exhibited a rapid propagation of the diagonal crack with little increase in the applied load which then marked the ultimate load carrying capacity of the slab. This implies that the ultimate load was not significantly increased beyond the first diagonal cracking load. On the contrary, the slabs reinforced with WWM or fibers continued to resist greater loads beyond that for the first diagonal cracking which led to a significant increase in the ultimate load of the fiber or WWM - reinforced slabs relative to the control slab. This can be attributed to the ability of fibers or WWM to bridge the diagonal cracking, to slow down the crack propagation, and distribute the stress to wider areas within the slab, thereby leading to a higher ultimate load carrying capacity relative to the control slab. Furthermore, the control slab exhibited rapid degradation in the load carrying capacity after the peak load was reached, while the slabs reinforced with fibers or WWM exhibited a steady state response after the ultimate load as reflected in the load deflection curves. This steady state response was associated with multiple diagonal cracking which also showed the enhanced ductility that fibers or mesh can impart into the composite deck slab.

The results of the load deflection behavior indicate that the level of enhancement depends on the type and extent of the reinforcement. For this purpose, two categories were identified: slabs reinforced with heavy WWM or relatively high dosage of fibers and slabs reinforced with moderate size WWM or low dosage of fibers. The first category includes the slabs reinforced with A142 mesh, 5.3 kg/m³ of synthetic macro-fibers, and 15.0 kg/m³ of steel fibers, while the second category includes the slabs reinforced with A98 mesh or 3.0 kg/m³ of synthetic macro-fibers. The load deflection response of the slabs of the first category as depicted by their respective curves shown in Fig. 6, shows that these slabs responded to the applied load in a quite similar manner and marked a greater ultimate load carrying capacity than the control slab. These slabs also exhibited similar post-peak behavior and sustained the peak load for a wider range of in-plane deflection

compared to that for the control slab. The post-peak behavior of these slabs was characterized by multiple diagonal cracking which contributed toward the improved ductility as reflected in the load deflection behavior. In contrast, the addition of 3.0 kg/m^3 of synthetic macro-fibers and the use of A98 mesh have led to just a slight increase in the ultimate load carrying capacity relative to the control slab (290 kN for control, 311 kN for the A98 mesh-slab, and 303 kN for the fiber-reinforced slab). However, the post-peak behavior was improved as indicated by the load deflection behavior. The slabs with A98 mesh and the one with 3.0 kg/m^3 of synthetic macro fiber exhibited similar behavior and sustained the ultimate load for greater in-plane deflection. Additionally, the rate of degradation in the strength was smaller relative to the control slab.

Overall, the load versus in-plane deflection response reveals the improvement in the global in-plane shear behavior that discrete fibers and WWM add to composite deck slabs relative to the control slab. This improvement is manifested in the first diagonal cracking load, the ultimate in-plane load carrying capacity and the ductility of the diaphragm slabs.

3.2 Ultimate in-plane shear capacity

The load-deflection results presented in the previous section show that fibers and WWM (specifically when high dosages of fibers or large mesh sizes are used) can impart significant improvement to the ductility of the slabs relative to the control specimen. Furthermore, the ultimate capacity of the diaphragm slab has been improved as reflected in the maximum sustained load. Table 2 presents the maximum in-plane load sustained by the slabs for all the specimens as well as the percentage increase in the ultimate capacity of the diaphragm slabs reinforced with fibers or mesh relative to the control specimen.

The results in the weak direction show that the addition of A142 mesh and that of 3.0 kg/m^3 and 5.3 kg/m^3 of synthetic macro-fibers increased the ultimate in-plane strength of the diaphragm slab by 9%, 38%, and 50%, respectively, suggesting that in the weak direction, synthetic macro-fibers imparted higher in-plane shear capacity.

On the other hand, test results in the strong direction indicate that the use of 3.0 kg/m^3 of synthetic macro-fibers and that of A98 mesh increased the ultimate in-plane shear capacity of

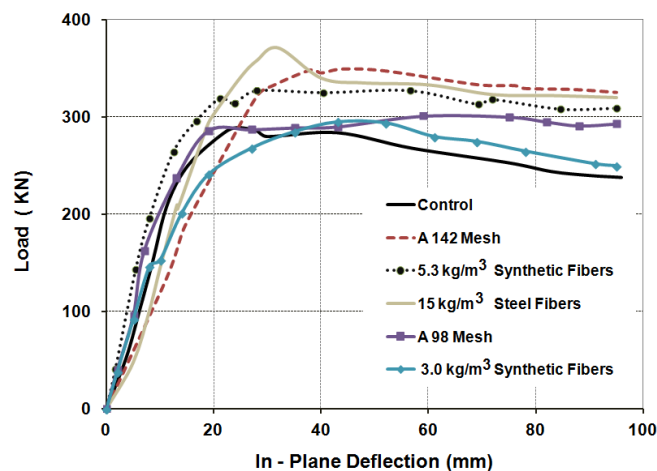


Fig. 6 Load-deflection response for slabs tested in the strong direction

Table 2 Increase in ultimate load

Test	Label	Secondary reinforcement	Concrete mix	Test configuration	Normalized ultimate load	Increase in ultimate load (%)
1	C-S	Control-no reinforcement	Mix 1	Strong	290	-
2	M ₁₄₂ -S -a	A142 mesh	Mix 1	Strong	338	16
3	M ₁₄₂ -S -b	A142 mesh	Mix 1	Strong	354	22
4	SN _{5.3} -S -a	5.3 kg/m ³ of Synthetic fibers	Mix 3	Strong	365	26
5	SN _{5.3} -S -b	5.3 kg/m ³ Synthetic Fibers	Mix 3	Strong	331	14
6	M ₉₈ -S	A 98 WWF mesh	Mix 1	Strong	311	7
7	SN _{3.0} -S	3.0 kg/m ³ Synthetic fibers	Mix 2	Strong	303	4
8	DR ₁₅ -S	15 kg/m ³ Steel fibers	Mix 4	Strong	374	29
9	C-W-R	Control	Mix 1	Weak	148	-
10	M ₁₄₂ -W	A142 mesh	Mix 1	Weak	161	9
11	SN _{5.3} -W	5.3 kg/m ³ Synthetic fibers	Mix 3	Weak	221	50
12	SN _{3.0} -W	3.0 kg/m ³ Synthetic fibers	Mix 2	Weak	205	38

the slabs relative to the control specimen by 4% and 7%, respectively. Similarly, the use of A 142 mesh, 5.3 kg/m³ of synthetic macro-fibers and that of 15.0 kg/m³ of steel fibers increased the ultimate in-plane shear capacity of the slab relative to the control by 19%, 20%, and 29%, respectively. These results suggest that A142 mesh, synthetic macro-fibers at the dosage rate of 5.3 kg/m³ and steel fibers at the dosage rate 15 kg/m³ can provide comparable improvements to the in-plane shear ultimate strength in the strong direction, and thus can be viewed as equivalent secondary reinforcements. Tantamount, A98 mesh and synthetic macro-fibers at the dosage rate of 3.0 kg/m³ can provide comparable improvements to the diaphragm strength under in-plane shear.

3.3 Analytical in-plane shear capacity

As will be addressed later in the cracking pattern, all the slabs tested in the strong direction failed through developing diagonal tension cracks. Thus, to further assess the test results, an analytical model predicting the shear strength of composite deck slabs controlled by diagonal tension is used. The model was presented by Easterling and Porter (1988) as given in Eq. (1) and is based on the ACI equation for the strength of shear walls (ACI 318-89). Treatment of shear walls and diaphragm effect in the recent editions of ACI remains appreciably similar (ACI 318-11).

$$V = 3.2t_e b \sqrt{f'_c} \quad (1)$$

Where, f'_c : concrete compressive strength in psi; t_e : effective slab thickness in inches; and b : diaphragm depth in inches.

The effective thickness t_e is considered to be contributed by both the steel deck and the concrete and is given by

$$t_e = t_c + n_s t \left[\frac{P}{P'} \right] \quad (2)$$

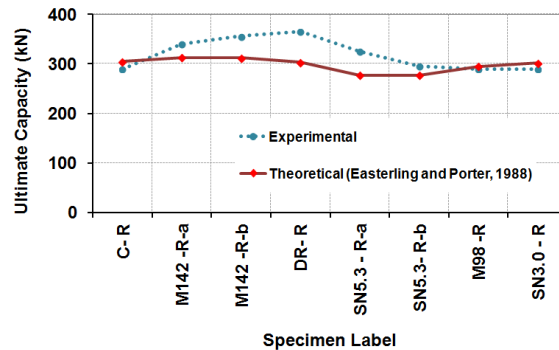


Fig. 7 Experimental vs. theoretical value of diaphragm ultimate in-plane shear

Where t_c : average concrete thickness considering the ribbed geometry; n_s : shear modular ratio of steel deck to concrete; t : steel sheet thickness; p : pitch (or spacing) of one deck rib; and p' : developed sheet width of one deck rib (sheet width of one deck rib taking into account the bend allowance). Schematic diagram for these parameters are previously shown in Fig. 3(c).

The above model (Eq. (1)) was used to evaluate the theoretical values of the in-plane shear strength of composite slabs tested in the strong direction and a comparison between experimental and theoretical values is presented in Fig. 7. Results reveal that the experimental and theoretical values of in-plane shear strength of composite slabs were quite coterminous for the control slab, the slab with A98 mesh and the one with 3.0 kg/m^3 of synthetic macro-fibers. Conversely, for the slabs with A142 mesh, 5.3 kg/m^3 of synthetic macro-fibers, and 15.0 kg/m^3 of steel fibers the experimental values were higher than the theoretical ones.

Based on the test results, while this model predicts well the diaphragm capacity controlled by diagonal tension for composite deck slabs with no or with light secondary reinforcement, it underestimates the shear strength of composite slabs involving heavy secondary reinforcement (A142 mesh; synthetic macro-fibers at 5.3 kg/m^3 , and steel fibers at 15.0 kg/m^3). This elucidates that although secondary reinforcement (WWM or Fibers) in composite metal decking is intended to control temperature and shrinkage cracks, its presence contributes to the in-plane shear capacity of the composite deck slabs. This contribution however, is not clearly incorporated by the current design practices and thus further investigations may be deemed necessary to help refining the current design guidelines for composite metal decks.

3.4 Load-strain responses

The measured strains in this study were used primarily to judge the type of failure of the diaphragm (i.e., shear failure versus flexural failure), to explain the cracking pattern, and to approximate the load at which debonding and shear cracking started. These measurements were also used to further explain the difference in behavior between the control and fibrous composite deck slabs.

3.4.1 Weak configuration

The strains in concrete were captured at different locations within the slab. As diagonal cracking was not observed in the slabs tested in the weak direction; cracks typically initiated over

the deck flute, and thus the slabs recorded much lower ultimate loads compared to their counterparts. Nonetheless, the effect of fibers on improving the diaphragm behavior in the weak direction relative to the control specimen was significant and can be explained from the strain data measured by gages 2 and 3 depicted in Figs. 8(a) and (b), respectively.

The load-strain results of Fig. 8(a) show that gage 2 measured relatively low tensile strain in the control slab (up to a load level of around 20 kN), after which the gage did not measure further tensile strain until failure, which indicates that the control slab lost its integrity at a very small load level. Likewise, the tensile strain measured by gage 3 (Fig. 8(b)) for the control slab was also very minimal which also supports the results obtained from gage 2. On the contrary, gages 2 and 3 continued to capture tangible tensile strain in the slab with synthetic macro-fibers at the dosage rates of 5.3 kg/m³ and 3.0 kg/m³, until load levels as high as 170 kN and 230 kN, respectively were reached. These results suggest that synthetic macro-fibers have improved the integrity of the diaphragms in the weak direction relative to the control.

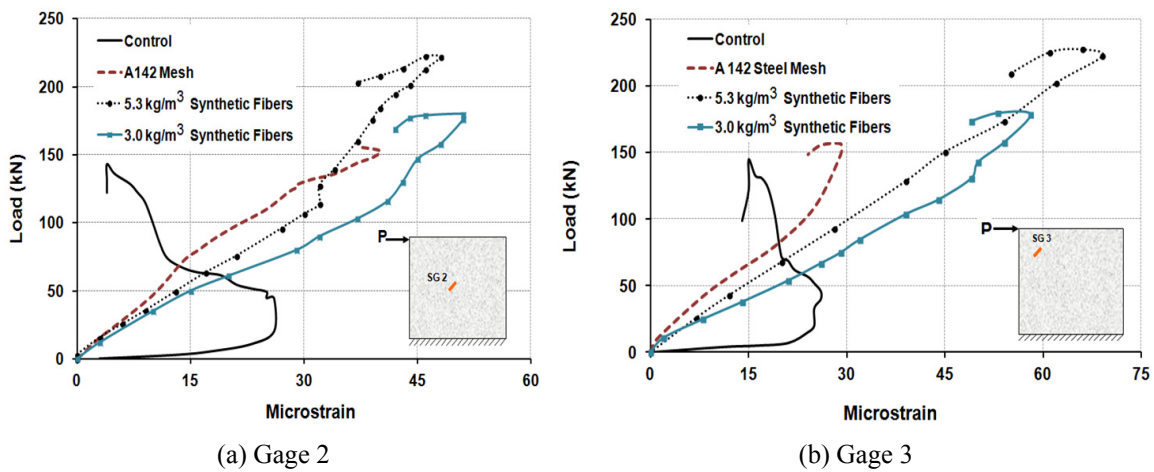


Fig. 8 Strain response for slabs tested in the weak direction

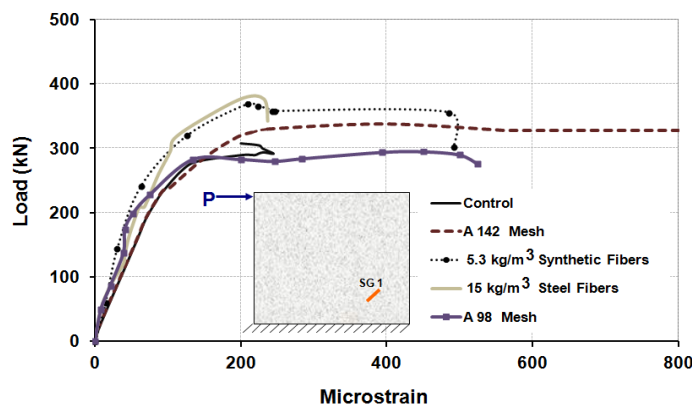


Fig. 9 Strain response captured by gage 1 in slabs tested in the strong direction

3.4.2 Strong direction

For the slabs tested in the strong configuration, the strain captured by gage 1 in the control slab; the slabs with A142 and A98 mesh; the slab with 5.3 kg/m^3 of synthetic macro-fibers; and the one with 15 kg/m^3 of steel fibers are presented in Fig. 9. It shows that the gage in all slabs responded linearly until the load at which the shear crack initiated (around 200 kN), after which the gage exhibited an unloading response for the control slab which experienced a rapid propagation of the shear crack and faster degradation of load carrying capacity. On the contrary, gage 1 in the slabs reinforced with A142 mesh, A98 mesh 5.3 kg/m^3 of synthetic macro-fibers, and 15 kg/m^3 of steel fibers continued to measure strain until the maximum load level was reached at which the gage showed either an unloading response or an extended mode depending on the orientation of the crack relative to the gage. This indicates that fibers and WWM both slowed down the crack propagation after initiation which led to higher load carrying capacity and further development of the multiple cracking observed in the strong configuration test.

3.4.3 Composite action and deterioration of interfacial bond

Another important aspect which can be explained by the strain data is the load at which debonding initiated between the concrete topping and the metal deck. The composite action at the interface between the profiled steel sheet and the concrete plays an important role in the shear transfer mechanism and thus in the integrity of the composite deck slab.

The strain at the interface has been captured by a pair of strain gages attached to the steel sheet and the concrete topping at key locations in the slab. The first was placed on the top surface of the deck flute to measure the strain in the steel sheet at the interface, while the second was positioned on the top surface of the concrete right above the first gage to measure the strain in the concrete. Schematic layout of these strain gages was shown earlier in Fig. 4(b). Readings from each pair of gages were collected and the load at which the interfacial bond degrades was identified based on the fact that each pair of identical strain gages at one location should theoretically record similar strain- with the assumption that the strain variation across the depth of the slab is subtle. When the steel sheet debonds from the concrete topping, a drastic variation in the strain record should be noticed between the two gages. Strain results measured by gages 3 and 6 are shown in Fig. 10 for the slabs with WWM and fibers. The examination of the strain response at the interface shows that the load levels corresponding to the deterioration of the interfacial bond and consequently the occurrence of debonding are linked to the formation of diagonal cracks in the composite deck slab; the reason for which only the slabs tested in the strong direction manifested the degradation of the interfacial bond as they failed through developing diagonal cracking due to the high load induced in that direction.

For instance, test observation show that the first diagonal tension crack in the slabs with A142 mesh, 5.3 kg/m^3 of synthetic macro-fibers, and 15.0 kg/m^3 of steel fibers developed at load levels of approximately 205 kN, 198 kN, and 202 kN, respectively. This can be confirmed from the slight change in the slope of the corresponding load deflection curves shown in Fig. 6. On the other hand, Fig. 10 depicting the strain at the steel-concrete interface shows that strain gages 3 and 6 recorded concurrent data in all three specimens up to a load level of approximately 200 kN, after which drastic divergence in reading was manifested, suggesting that deterioration of the interfacial bond (leading to failure in shear transfer mechanism due to loss of composite action) has occurred. This happened at a similar load level that caused the formation of diagonal tension cracking. However, regardless of the reinforcement typology, the results showed that all the three secondary

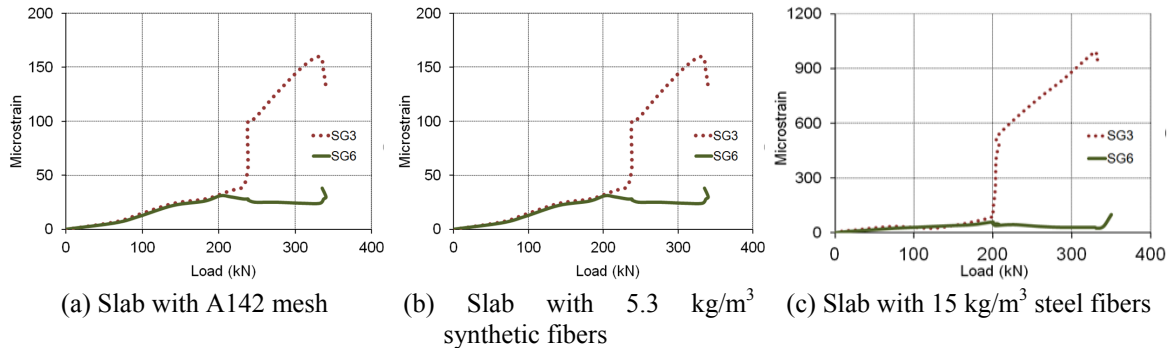


Fig. 10 Interfacial strain response

reinforcement systems (synthetic fibers, steel fibers and WWM) exhibited a similar load level at which the interfacial bond degraded. This suggests that these reinforcement systems at the tested fiber dosages and mesh sizes have a comparable effect on the shear transfer mechanism in composite deck slabs.

3.5 Cracking and failure mode

Cracking pattern and sequence were carefully monitored and mapped during testing. Fig. 11 presents pictures of cracking pattern and sequence for the control and the slabs reinforced with fibers or mesh. Two types of failure patterns were identified depending on the test configuration: diagonal tension cracking in the strong direction and flexural cracking over the deck flute in the weak direction. Test Observations reveal that all slabs tested in the strong direction failed by developing diagonal tension cracks, but the number and severity of cracks at failure were dependent on the type of reinforcement used in the composite deck slab. The control slab was characterized by a single diagonal crack (Fig. 11(a)) which subsequently widened up as the peak load was approached. The post peak strength of the control slab was characterized by a rapid degradation associated with widening and propagation of the diagonal crack. Conversely, the FRC slabs and the slab with WWM developed multiple diagonal shear cracks before failure (Fig. 11(b) and Fig. 11(c)). Furthermore, the formation of the first diagonal tension crack did not mark the failure of these slabs reinforced with either fibers or WWM as they continued to resist higher loads and developed more diagonal cracking before failure, which occurred in a gradual and stable manner. This cracking pattern is consistent with the load-deflection data discussed previously. The development of multiple diagonal shear cracks contributed to the increased ductility of the slabs observed in the load deflection curves. Moreover, the cracking pattern shows that fibers reduced splitting around the shear studs along the fixed edge of the diaphragm. This may be attributed to the fact that fibers improved the confinement stress around the studs and thus reduced splitting. This allowed for an effective transfer of load from the shear connectors to the reaction beam and consequently enhanced the overall performance and integrity of the diaphragm.

Unlike the slabs tested in the strong direction, the ones tested in the weak direction failed through developing flexural cracks over the deck flute (Fig. 11(d)) Diagonal cracking in the weak direction did not occur due to the flexural weakness of the composite slab over the deck flute, and the crack typically initiated over the deck flute for all slabs tested in the weak direction.

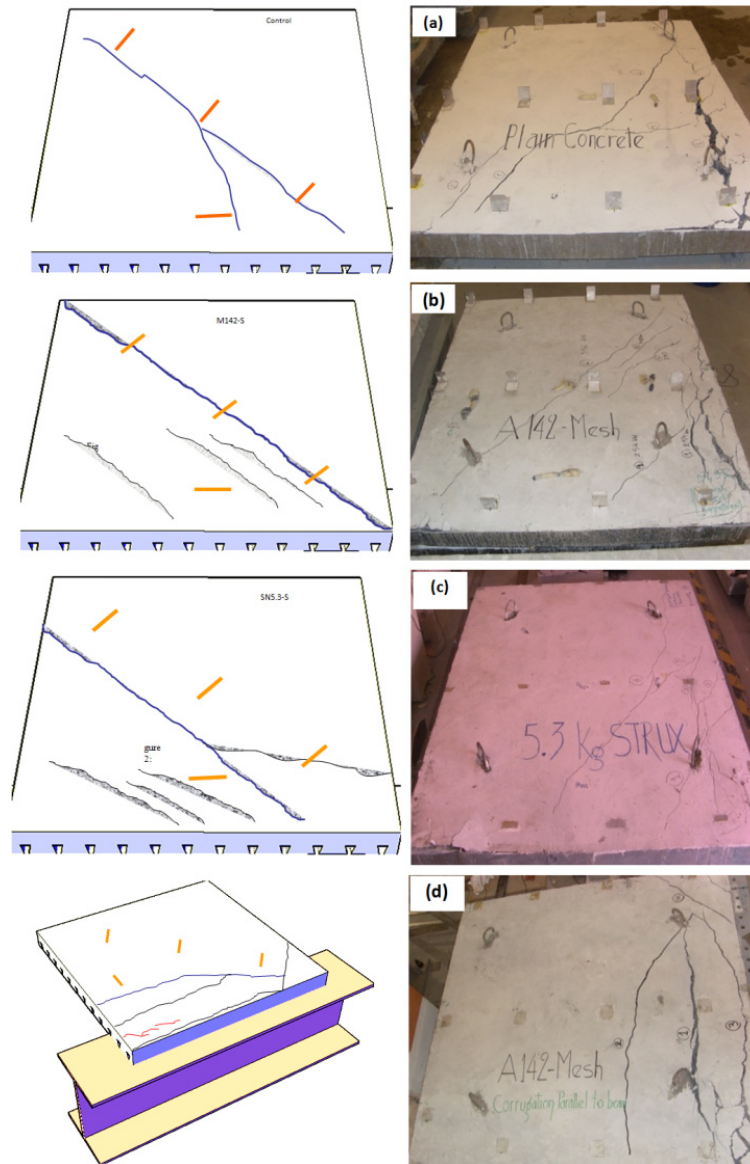


Fig. 11 Cracking and failure: (a) Control slab; (b) Slab with A142 steel mesh; (c) Slab with 5.3 kg/m^3 of synthetic fibers; (d) Slab with A 142 steel mesh tested in the weak orientation

4. Conclusions

In this study, twelve large-scale composite deck slabs were instrumented and tested in cantilever diaphragm configuration under monotonic loading to investigate the in-plane shear behavior of FRC composite deck slabs. The slabs were constructed with a reentrant decking profile and reinforced with different types of secondary reinforcement (steel mesh, synthetic fiber, and steel fiber). Load-deflection response and strains in the composite deck slab were measured

and the cracking pattern was reported. The results show that all slabs tested in the strong direction exhibited diagonal cracking while those tested in the weak direction exhibited the formation of cracks at the thin section above the flute deck and failed at lower loads than that for their counterparts. The load deflection results show that the addition of fibers and WWM increased the ultimate in-plane shear capacity and ductility of the slabs relative to the control. For the slabs tested in the strong direction, the use of A 142 mesh resulted in 19% increase in the ultimate in-plane shear capacity and the additions of 5.3 kg/m³ of synthetic macro-fibers and 15 kg/m³ of steel fibers increased the ultimate in-plane shear capacity by 20% and 29%, respectively.

The effect of fibers on the ultimate shear capacity of the diaphragm was more pronounced in the slabs tested in the weak direction. The results show an increase in the ultimate in-plane shear capacity of 38% and 50% when the synthetic fibers were added at dosage rates of 3.0 kg/m³ and 5.3 kg/m³, respectively. Conversely, the inclusion of A 142 mesh in the slab increased the ultimate capacity of the slab by only 9% relative to the control slab, suggesting a higher performance for fibers in the weak direction of the composite metal deck. Overall, the results show that fibers although used to control temperature and shrinkage cracks, have considerable impact on enhancing the in-plane shear capacity, hence can be viewed as viable secondary reinforcement in composite deck slabs. The strain results show that the initiation of the diagonal tension crack was associated with the deterioration of the interfacial bond between the steel deck and the concrete. The load level at which this phenomenon occurred was quite similar for all tested slabs suggesting that the secondary reinforcement typology does not affect the interfacial bond.

Comparison between the experimental results and an analytical model (based on diagonal cracking) reveals that the model does not reflect the contribution of secondary reinforcement to the diaphragm capacity, a remark consistent with the current design practice that overlooks this contribution. However, the results obtained in this study suggest that refinement of such current design guidelines may be deemed necessary to account for the significant contribution of the secondary reinforcement (fibers and WWM) to the diaphragm capacity.

In summary, the results of the load deflection response, the strain measurements, the ultimate in-plane shear capacity of the diaphragms, and the cracking and failure mode all indicate the viability of synthetic macro-fibers and steel fibers as secondary reinforcement in composite slabs and that fibers impart significant enhancement to the in-plane shear capacity and ductility of composite deck slabs comparable to that obtained using the traditional WWF mesh.

Acknowledgments

The authors would like to thank Emirates Stones Company Ltd, Sharjah for supporting this project during the construction stage. Special thanks are due to Eng. Jawdat Al Bargawi, the General Manager and Eng. Mohammed Ali, the Production Manager for their helpful cooperation. In addition, the authors want to express their gratitude to Grace Middle East, Dubai-UAE for providing the synthetic fibers and to Richard Lee Steel Decking, UK for supplying the steel decking.

References

- Abdullah, R. and Easterling, W. (2007), "Determination of composite slab strength using a new elemental test method", *J. Struct. Eng.*, **133**(9), 1268-1277.

- ACI Committee 544 (1982), State of the art report of fibre reinforced concrete; *Concrete Int.: Des. Construct.*, **4**(5), 9-30.
- ACI 318 (2011), Building code requirements for structural concrete and commentary; American Concrete Institute, Farmington Hills, MI, USA.
- Ahmat, H.O (2010), “Diaphragm behavior of fiber-reinforced composite deck slabs”, M.S. Thesis; University of Sharjah, Sharjah, UAE.
- AISC (2010), Manual of steel construction-load and resistance factor design; American Institute of Steel Construction Chicago, IL, USA.
- ASTM C 1609-07 (2007), Standard test method for flexural performance of fiber-reinforced concrete (using beam with third-point loading); ASTM International, West Conshohocken, PA, USA.
- BS EN ISO 898-1 (2009), Mechanical properties of fasteners made of carbon steel and alloy steel – part I, bolts, screws and studs with specified property classes – coarse thread and fine pitch thread; British Standards Institute, London, UK.
- BS EN 10147 (2000), Continuously hot-dip zinc coated structural steels strip and sheet; British Standards Institute, London, UK.
- BS 1881-101 (1983), Testing Concrete, Part 101: Method of sampling fresh concrete on site; British Standards Institute, London, UK.
- BS 1881-116 (1983), Testing Concrete, Part 116: Method for determination of compressive strength of concrete cubes; British Standards Institute, London, UK.
- Cifuentes, H. and Medina, F. (2013), “Experimental study on shear bond behavior of composite slabs according to Eurocode 4”, *J. Construct. Steel Res.*, **82**(2013), 99-110.
- Chen, S., Shi, X. and Qiu, Z. (2011), “Shear bond failure in composite slabs – A detailed experimental study”, *Steel Compos. Struct., Int. J.*, **11**(3), 233-250.
- Davies, J.M. and Fisher, J. (1979), “The diaphragm action of composite slabs”, *Inst. Civil Eng.*, **67**(2), 891-906.
- Easterling, W.S. and Porter, M.L. (1988), “Behavior, analysis and design of steel-deck-reinforced concrete diaphragms”, Final Report; Iowa State University, Engineering Research Institute - Project 1636, Ames, IA, USA.
- Easterling, W.S. and Porter, M.L. (1994), “Steel deck reinforced concrete diaphragms-I”, *ASCE J. Struct. Eng.*, **120**(2), 560-576.
- Easterling, W.S. and Young, C.S., (1992), “Strength of composite slabs”, *J. Struct. Eng.*, **118**(9), 2370-2389.
- Guirola, M. (2001), “Strength and performance of fiber - reinforced concrete composite slabs”, M.S. Thesis; Virginia Polytechnic Institute and State, VA, USA.
- Hossain, K.M.A. and Wright, H.D. (2004), “Experimental and theoretical behavior of composite walling under in-plane shear”, *J. Construct. Steel Res.*, **60**(1), 59-83.
- Hedao, N.A., Gupta, L.M. and Ronghe, G.N. (2012), “Design of composite slabs with profiled steel decking: A comparison between experimental and analytical studies”, *Int. J. Adv. Struct. Eng.*, **3**(1).
- James, L. and Easterling, W.S. (2006), “Structural performance of fiber reinforced and welded wire fabric reinforced composite slabs”, Research Report CEE/VPI – ST-06/05, Virginia Polytechnic Institute, VA, USA.
- JSCE-SF4 (1984), Methods of Tests for Flexural Strength and Flexural Toughness of Steel Fiber Reinforced Concrete; Japan Society of Civil Engineers, Concrete Library International, No. 3, Part III-2, pp. 58-61.
- Lopes, E. and Simões, R. (2008), “Experimental and analytical behaviour of composite slabs”, *Steel Compos. Struct., Int. J.*, **8**(5), 361-388.
- Luttrell, L.D. (1971), “Shear diaphragms with lightweight concrete fill”, *Proceedings of the 1st Specialty Conference on Cold-Formed Steel Structures*, University of Missouri-Rolla, Rolla, MO, USA, August.
- Luttrell, C.B. (1995), “Transverse distribution of non-uniform loads on composite slabs”, M.S. Thesis; West Virginia University, WV, USA.
- Porter, M.L. and Ekberg, C.E. Jr. (1978), “Compendium of ISU research conducted on cold-formed steel-deck reinforced slab systems”, Bull. 200-1978; ISU-ER1- AMES-78263, Engineering Research Institute, Iowa State University, Ames, IA, USA.

- Roesler, J.R., Altoubat, S.A., Lange, D.A., Rieder, K.A. and Ulreich, G.R. (2006), "Effect of synthetic fibers on structural behavior of concrete slabs-on-ground", *ACI Mater. J.*, **103**(1), 3-10.
- Saravanan, M., Marimuthu, V., Prabha, P., Arul Jayachandran, S. and Datta, D. (2012), "Experimental investigations on composite slabs to evaluate longitudinal shear strength", *Steel Compos. Struct., Int. J.*, **13**(5), 489-500.

CC